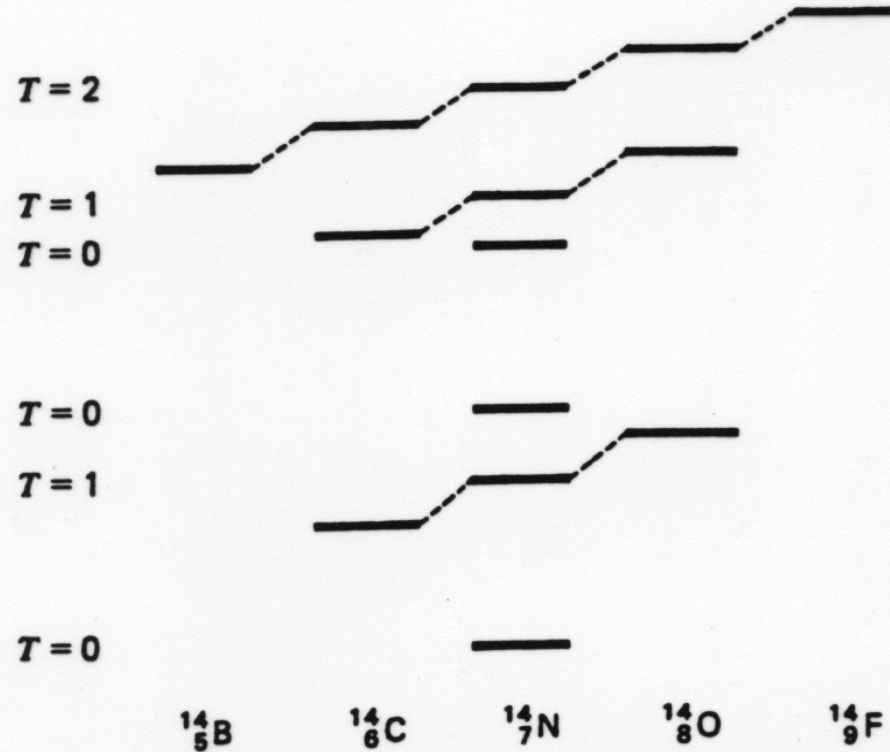


**Fig. 8.6.** Level structure in the two isobars  $^7\text{Li}$  and  $^7\text{Be}$ . These two nuclides contain the same number of nucleons; apart from electromagnetic effect, their level schemes should be identical.  $J^\pi$  denotes spin and parity of a level,  $I$  its isospin. Parity will be discussed in Chapter 9. [For reference see F. Ajzenberg-Selove, *Nucl. Phys.* **A490**, 1 (1988).]

$$E_{IA}(Z+1) = E_{IA}(Z) + \Delta E_c - (m_n - m_H)c^2, \quad (10-8)$$



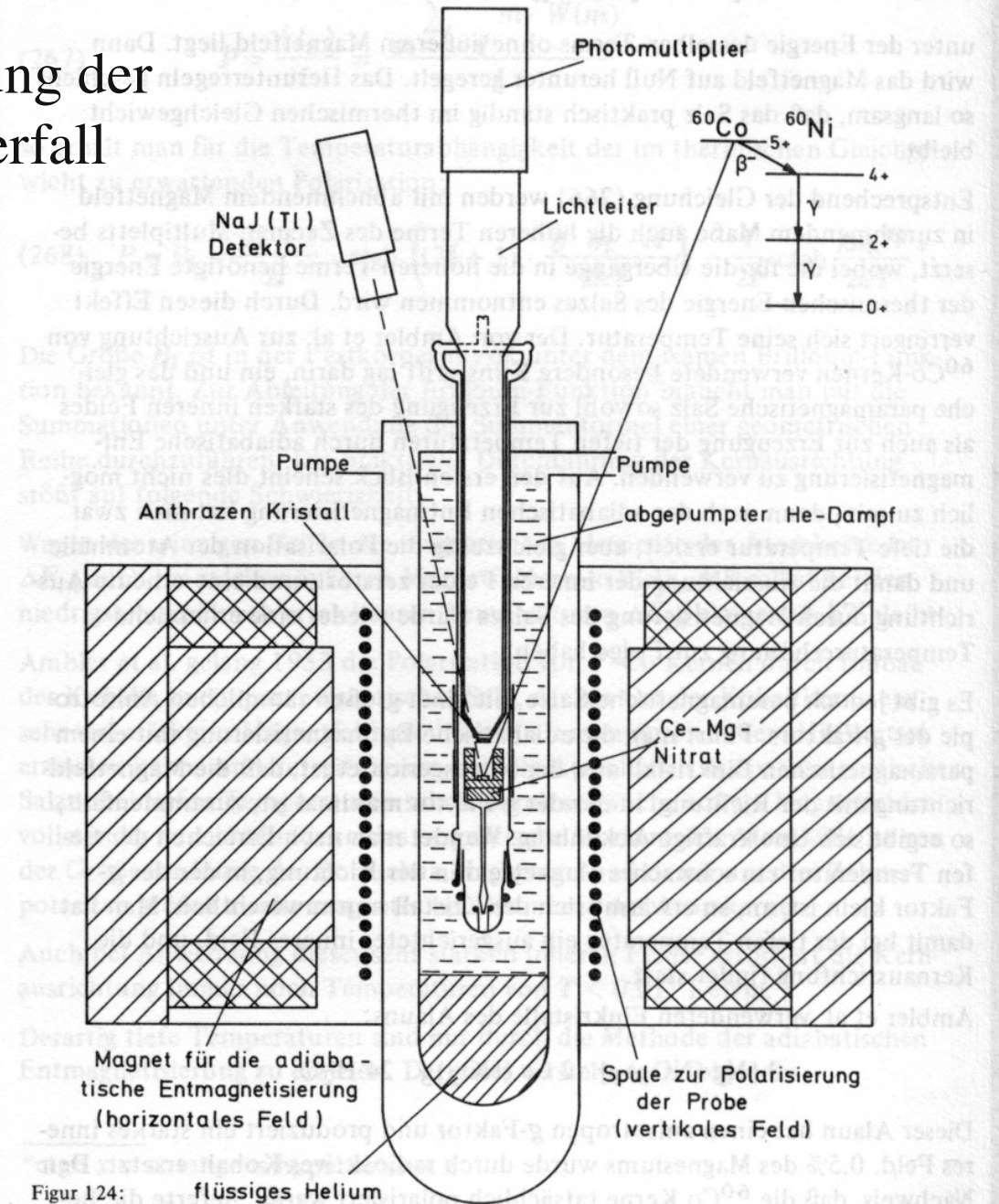
**Fig. 10-2** Isobaric analog states in  $A = 14$  nuclei. States are classified according to the  $T$  quantum numbers. [Adapted from *Concepts of Nuclear Physics* by B. L. Cohen. Copyright © 1971 by McGraw Hill, Inc. Used with the permission of McGraw Hill Book Company.]

$$T_{\min} = T_2 = 2 \quad 1 \quad 0 \quad 1 \quad 2$$

$$T_{\max} = 7 \quad 7 \quad 7 \quad 7 \quad 7$$

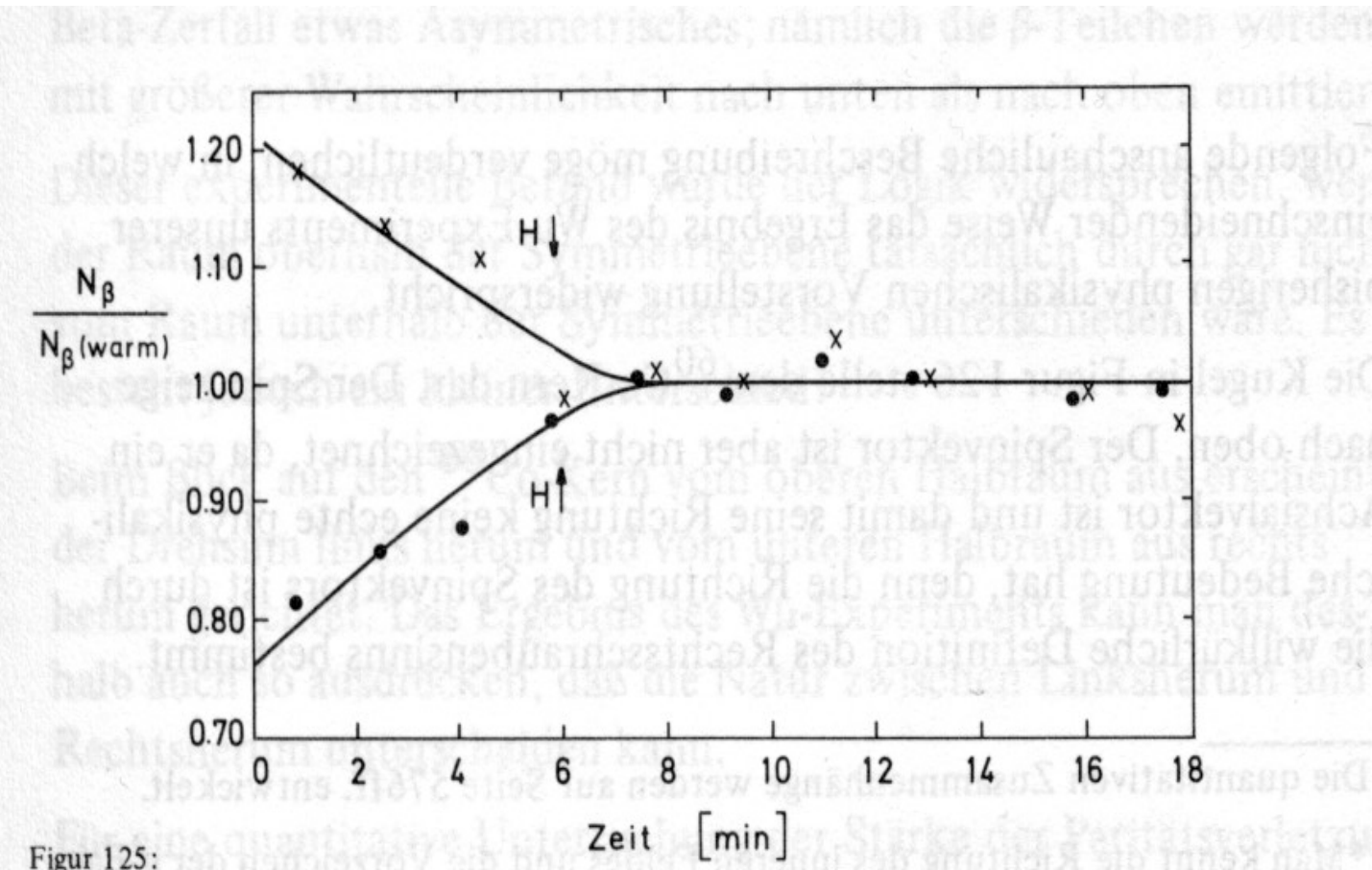
Fig. 4-2

# Wu Experiment zur Entdeckung der Paritätsverletzung im Beta-Zerfall



Figur 124: flüssiges Helium

Anordnung von Wu et al., Phys. Rev. 105, 1413 (1957) zur Beobachtung der Paritätsverletzung beim Beta-Zerfall.



Figur 125:

Beobachtete Beta-Zählrate als Funktion der Zeit in der Anordnung der Figur 111. Diese Meßkurve ist der Arbeit von Wu et al., Phys.Rev. 105, 1413 (1957) entnommen.

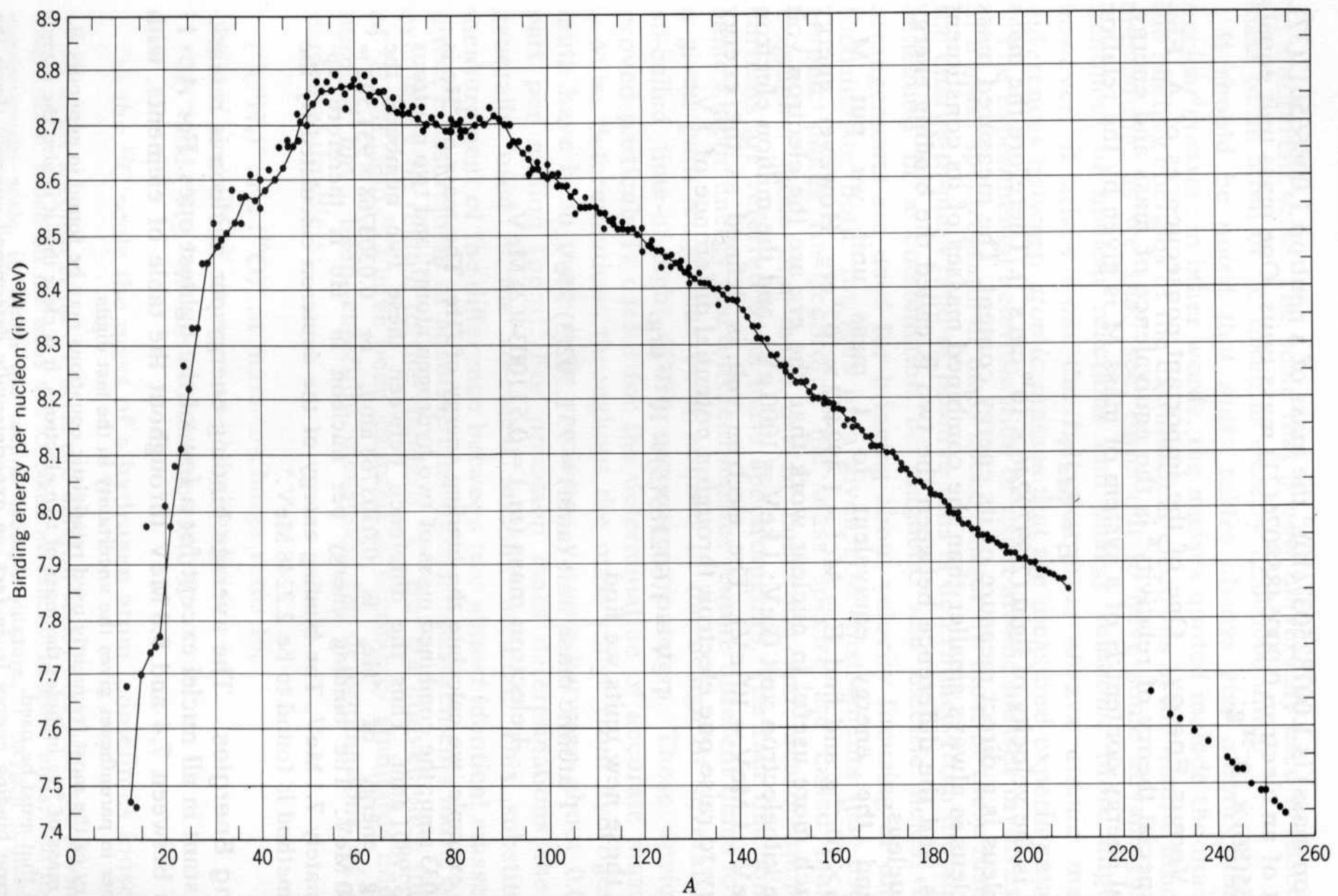


Fig. 5-1

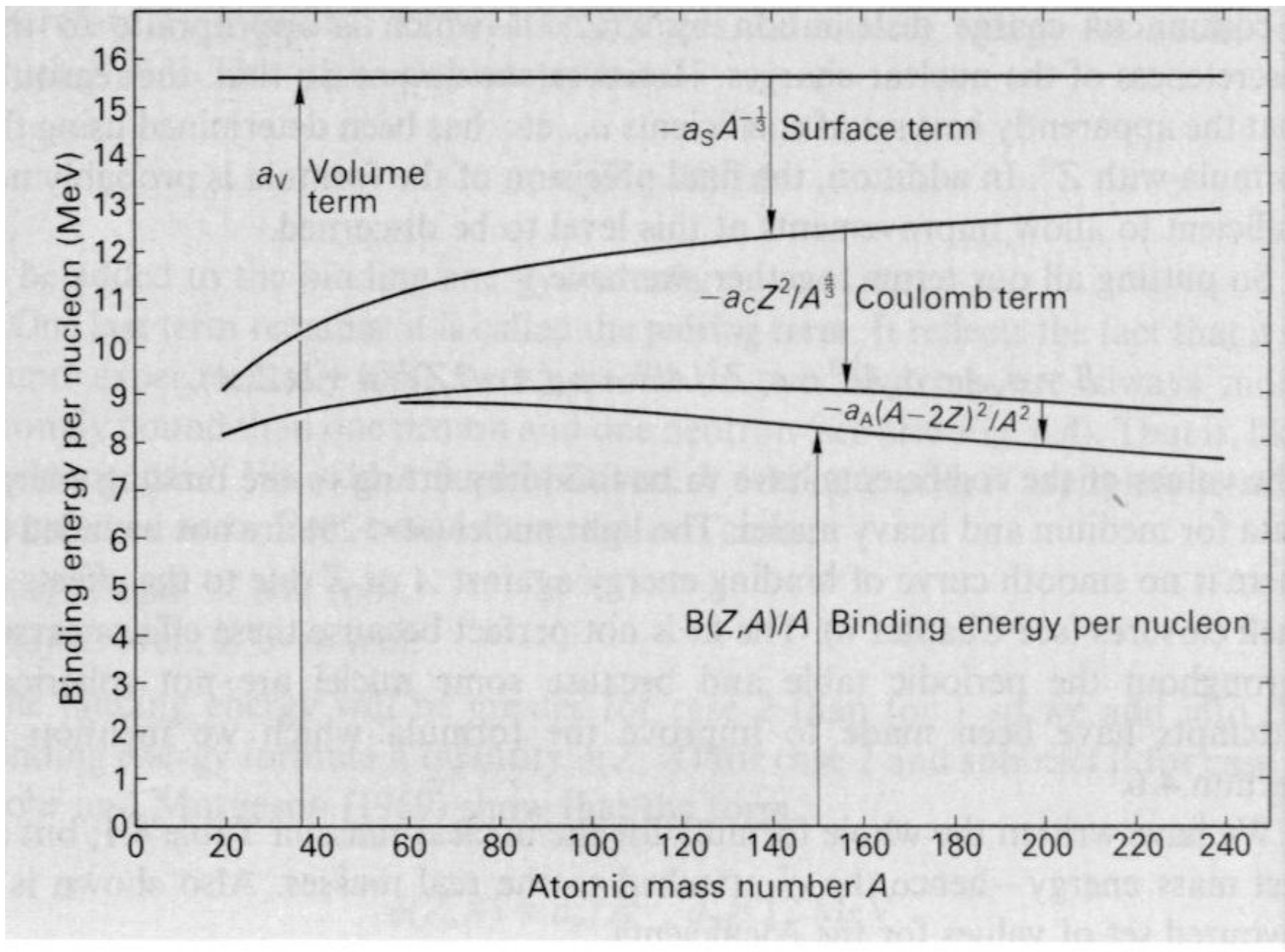


Fig. 5-2

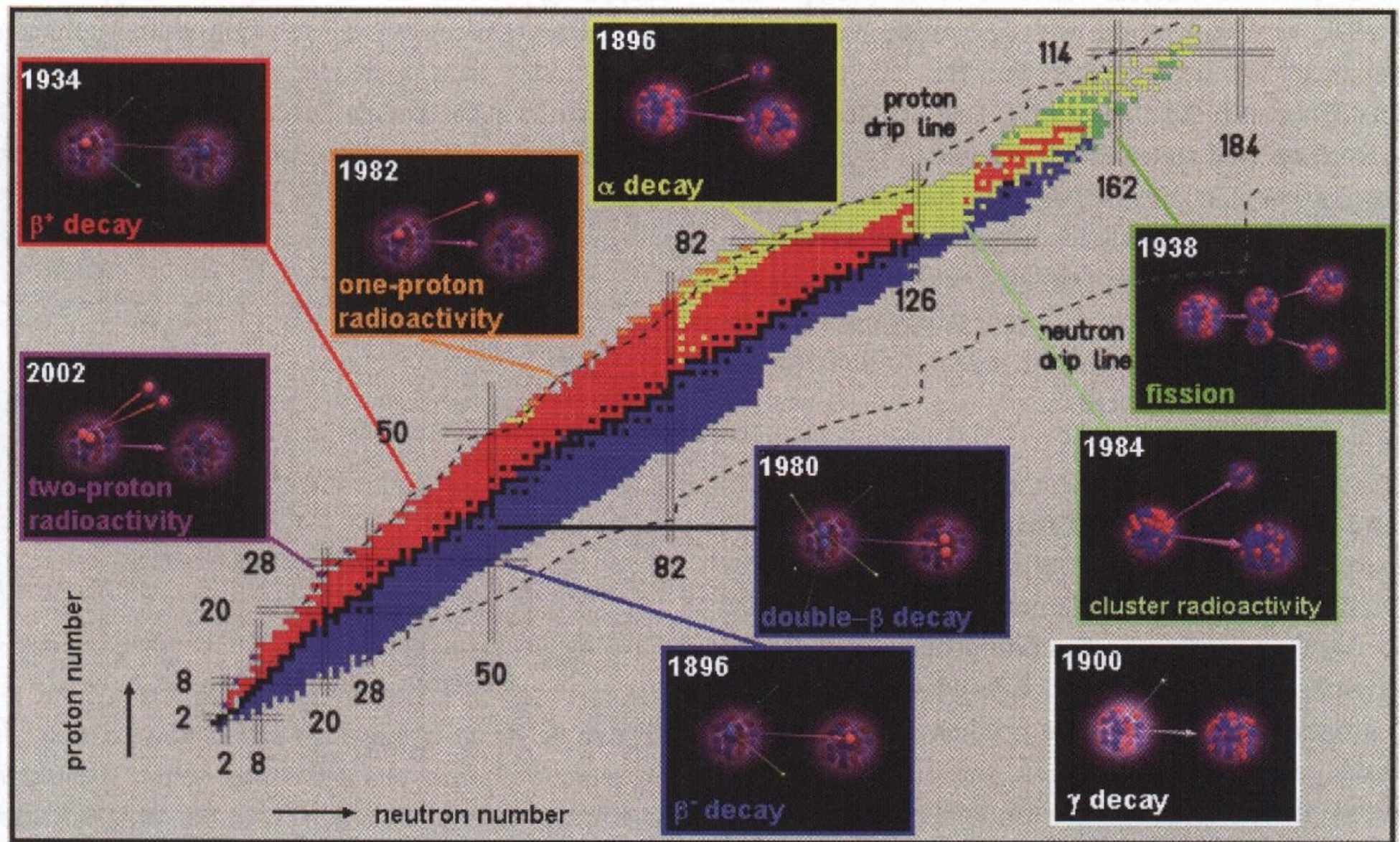
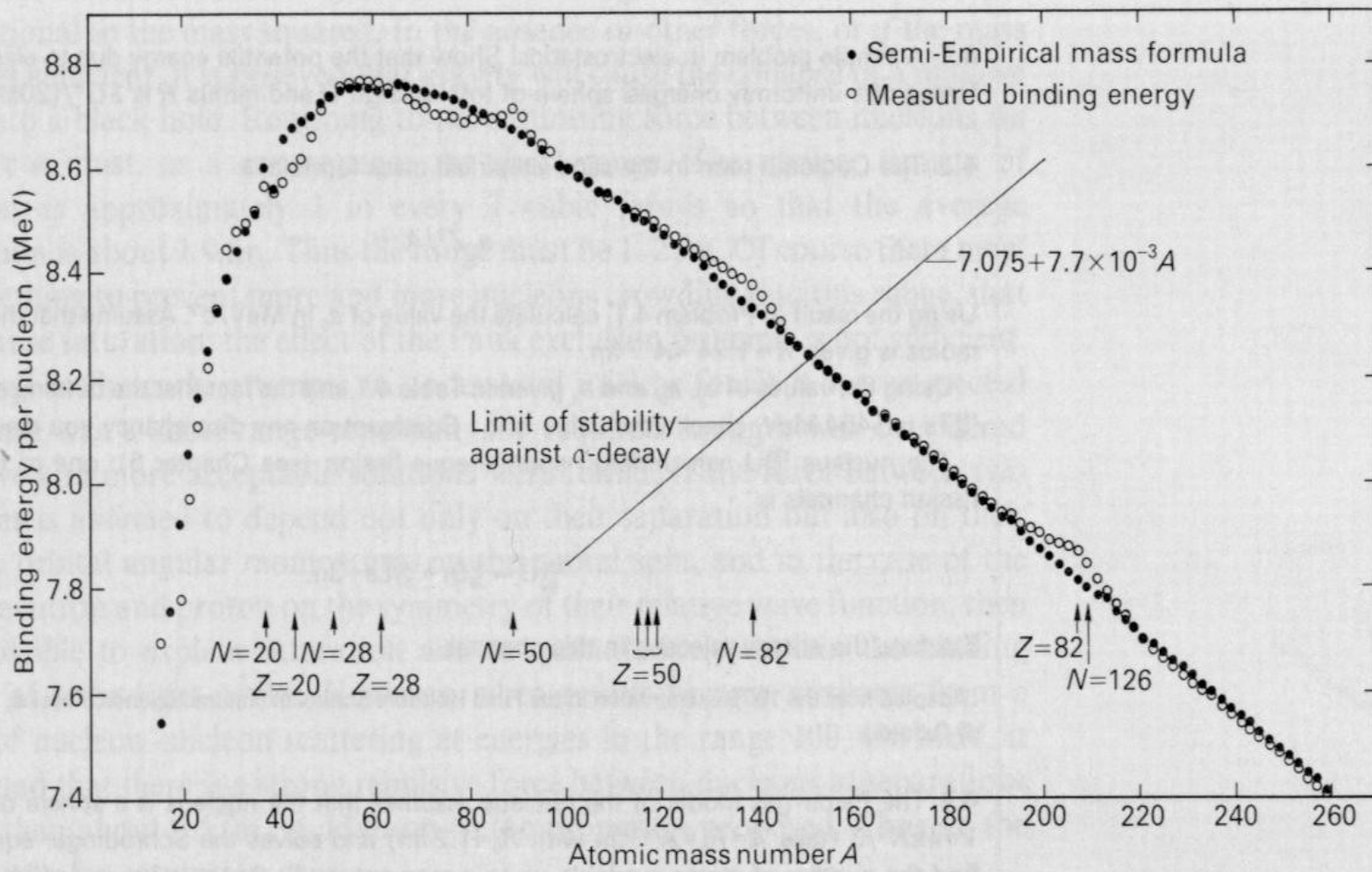
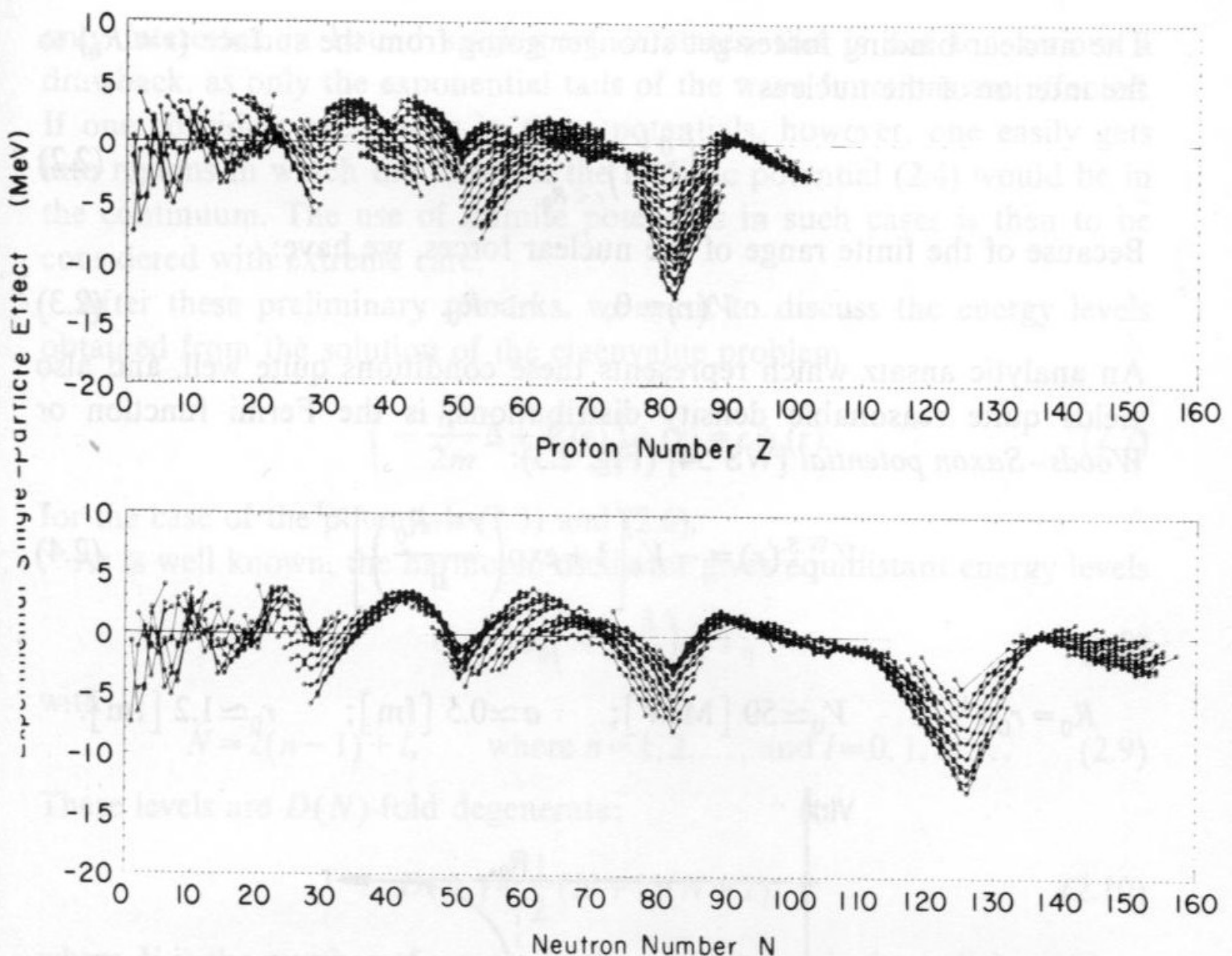


Fig. 5-2a



**Fig. 4.6** The binding energy as a function of  $A$  for the odd- $A$  nuclei from  $A = 15-259$ . The solid points are the prediction of the semi-empirical mass formula as given in Table 4.1. The open points are the measured values. The points for the formula do not lie on a smooth curve because  $Z$  for these nuclei is not a smooth function of  $A$  (see Fig. 4.1). Note that the zero

of the ordinate is suppressed and its scale is much enlarged. Thus, in spite of the deviations from the formula, it is clear that the formula predicts the binding energy per nucleon for  $A > 20$  with a precision which is, for the majority of cases, better than 0.1 MeV. The straight line crossing the curve at  $A = 151$  gives the limit of stability of nuclei to  $\alpha$ -decay (see Section 5.4).



**Figure 2.2.** Deviations of nuclear masses from their mean values plotted as a function of neutron and proton number. (From [MS 66].)

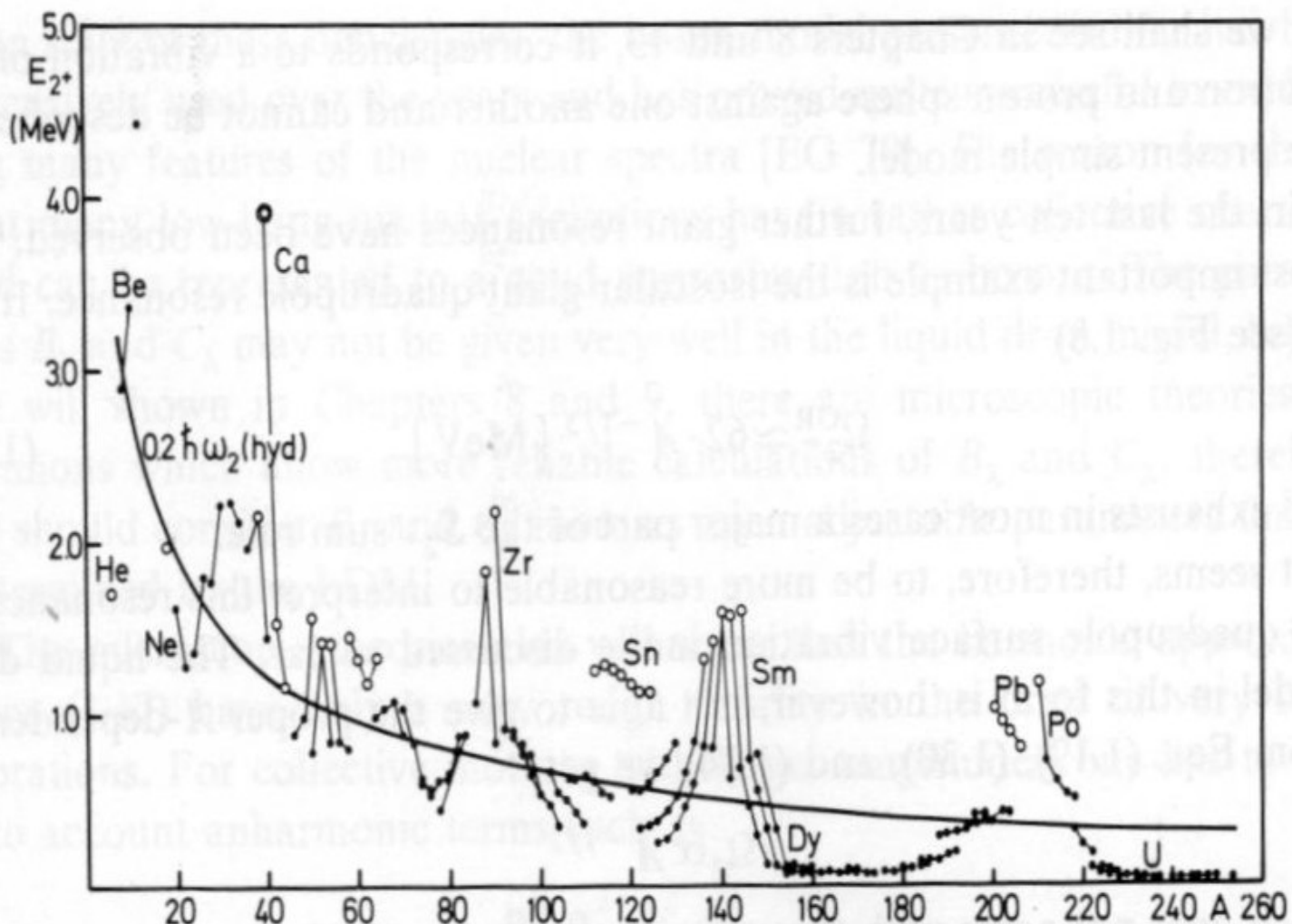


**Figure 1.7.** The energy of the first  $2^+$  state in even-even nuclei. The nuclei with closed neutron or proton shells are marked by open circles. (From [NN 65].)

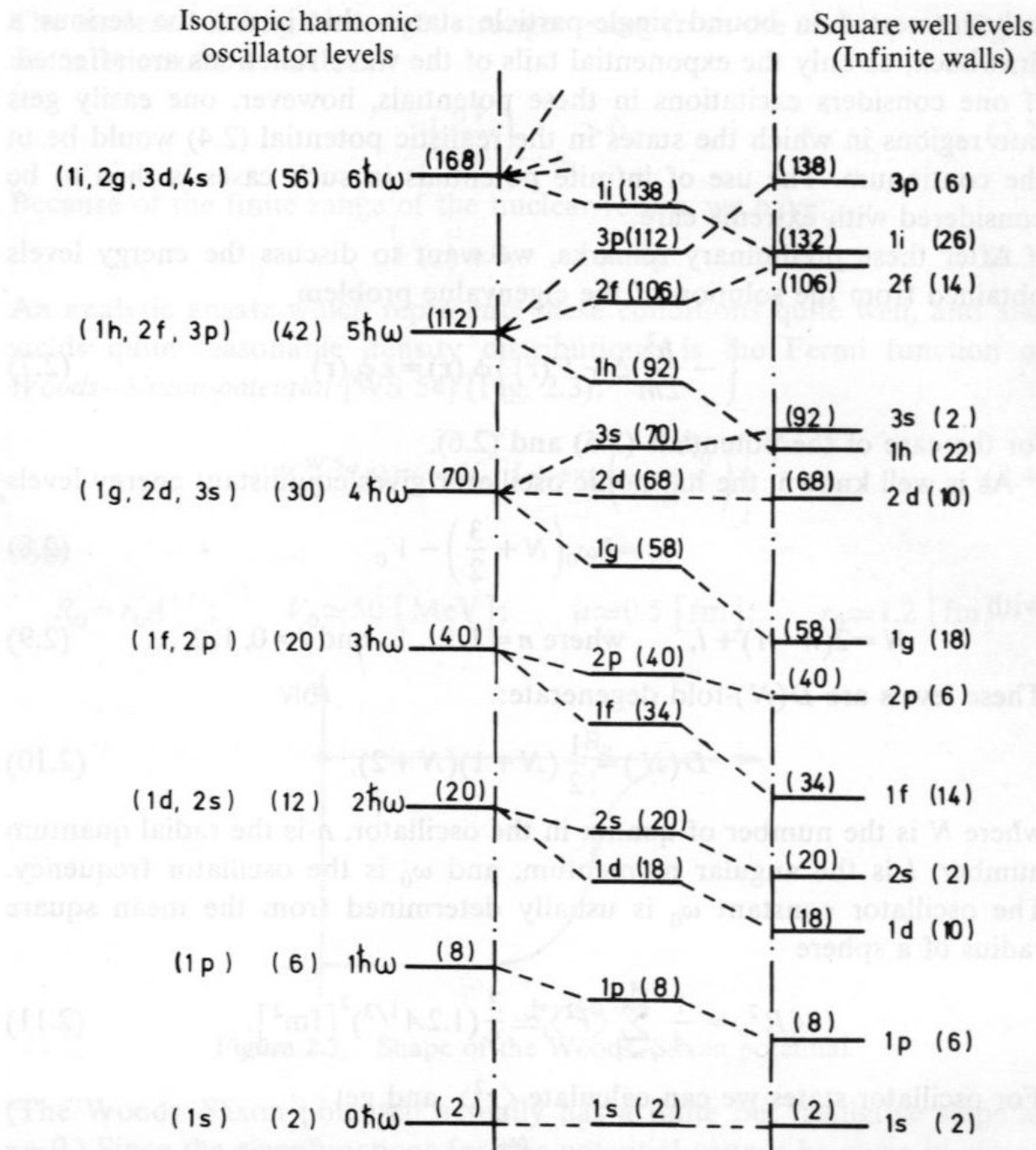


**Figure 2.4.** Level scheme of the isotropic harmonic oscillator (l.h.s.) and of the infinite square well (r.h.s.). (From [MJ 55]).

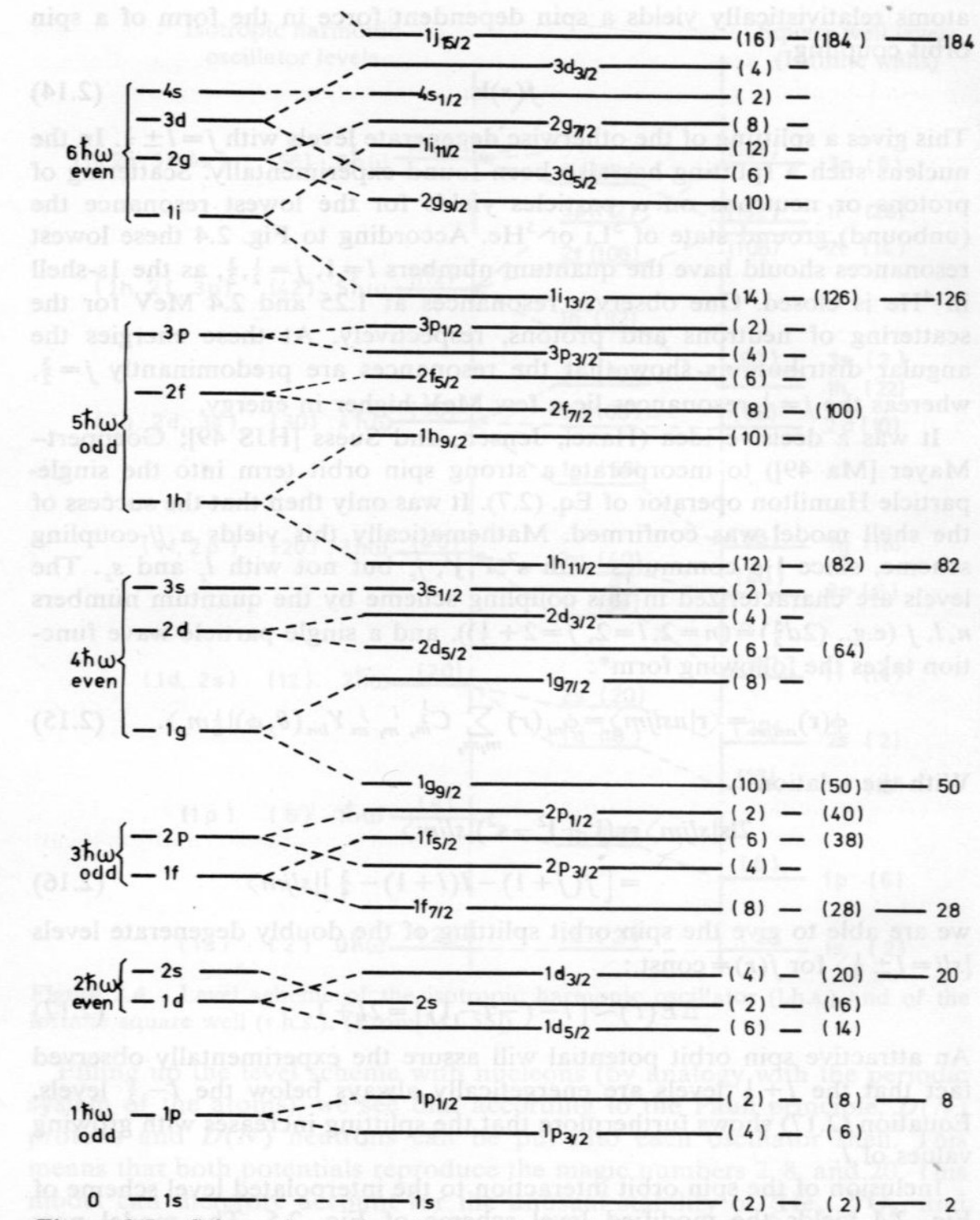


Fig. 5-7

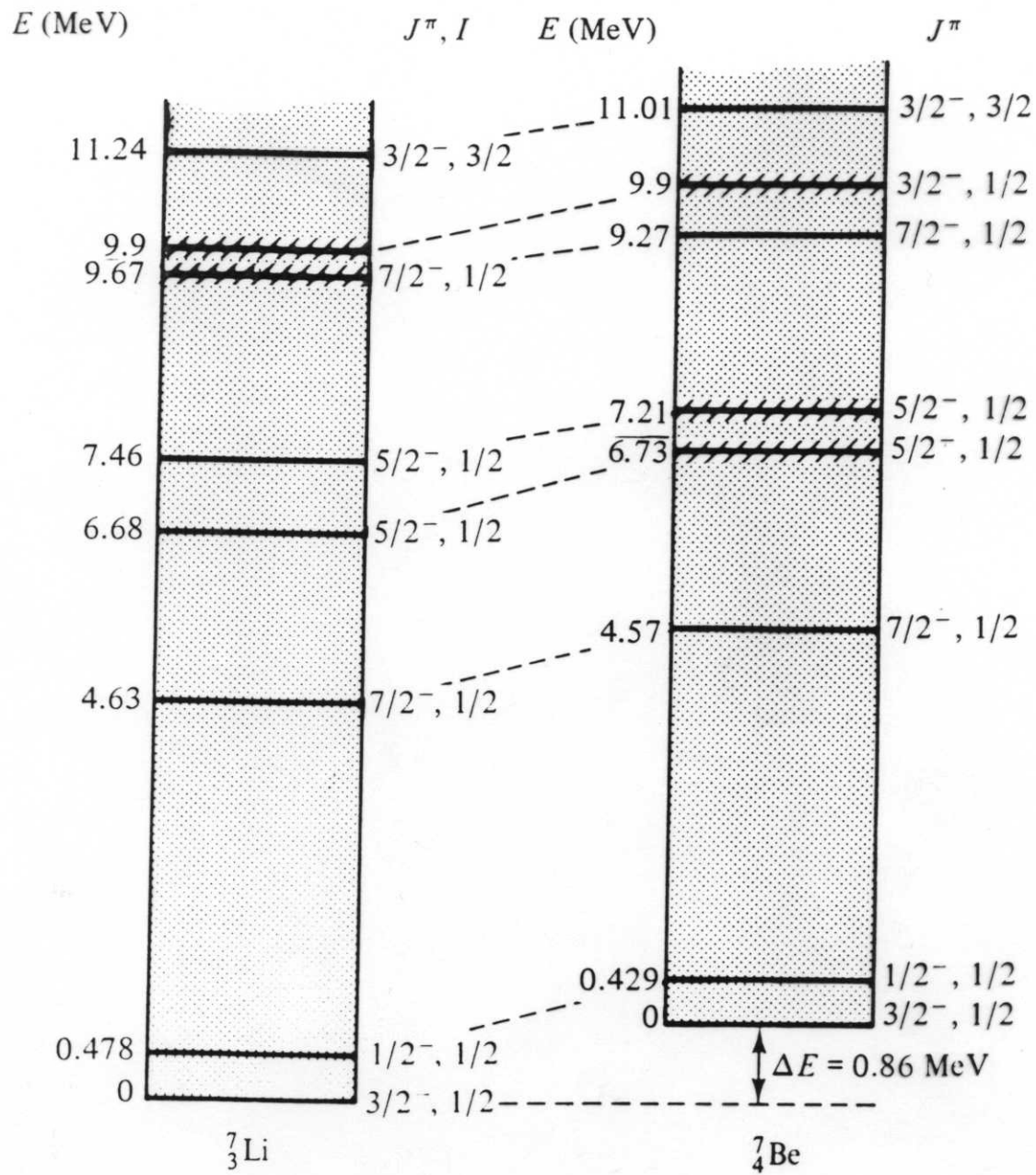


Fig. 5-8

# Spaltung von $^{235}\text{U}$ nach Neutroneneinfang

Figure 5-9 - Fission of a  $^{92}_{\text{U}}$  nucleus after capture of a neutron.

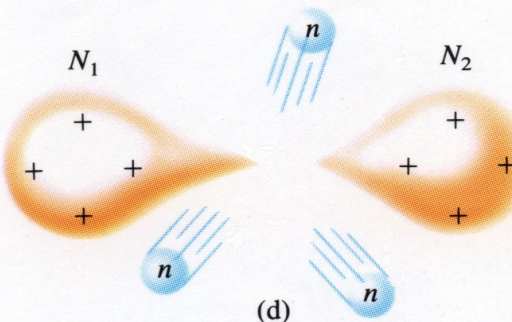
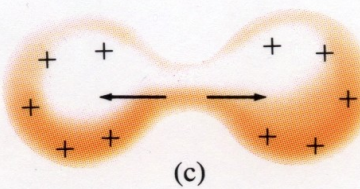
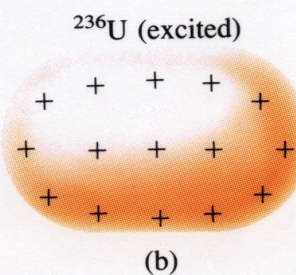
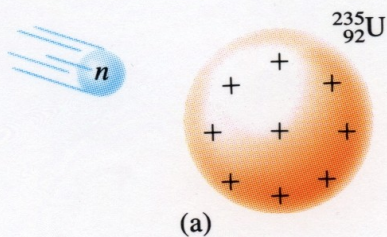
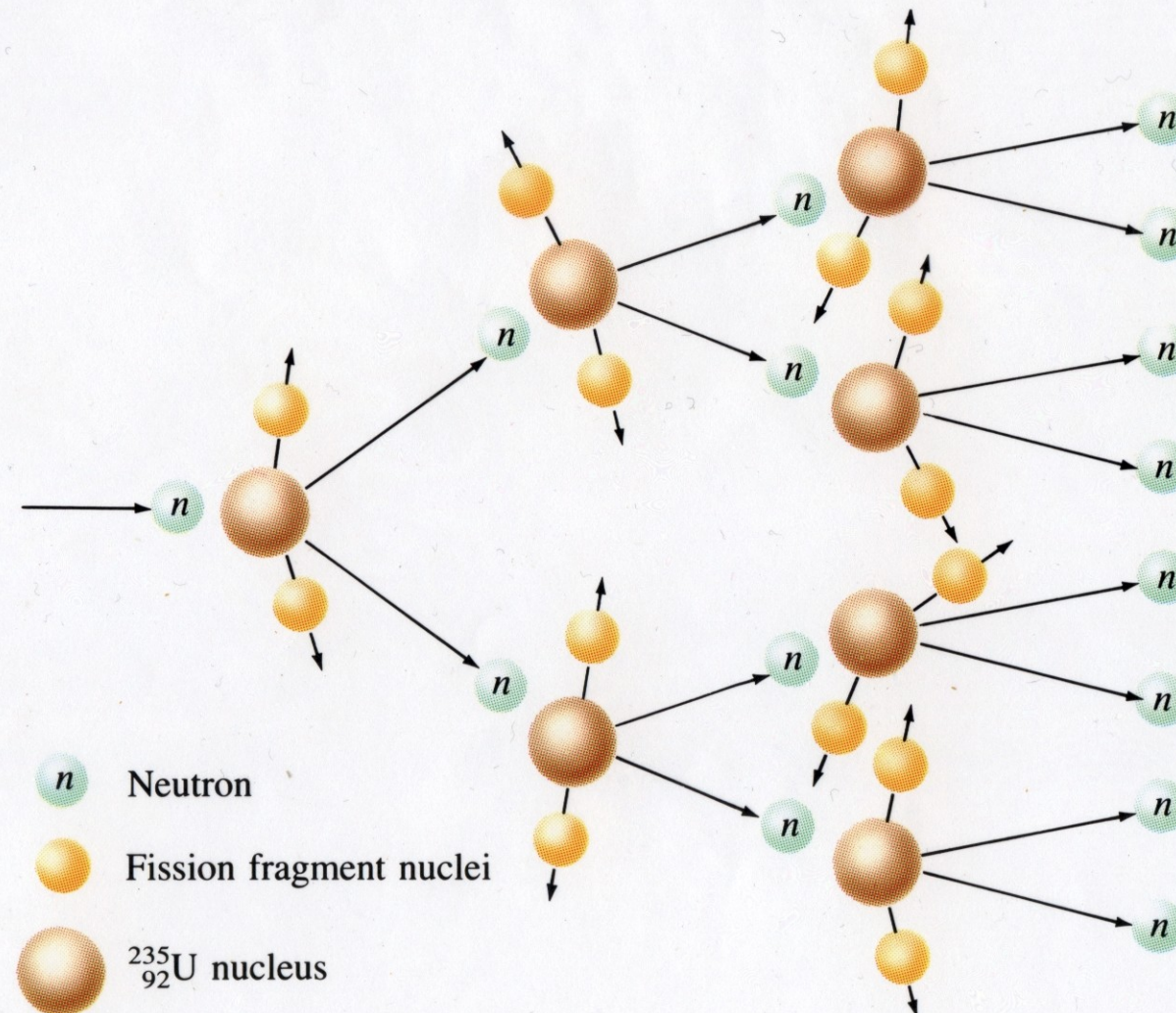


Fig. 5-9

## Prinzip der Kettenreaktion:





**FIGURE 31-4** Color painting of the first nuclear reactor, built by Fermi under the grandstand of Stagg Field at the University of Chicago. (There are no photographs of the original reactor because of military secrecy.) Natural uranium was used with graphite as moderator. On December 2, 1942, Fermi slowly withdrew the cadmium control rods and the reactor went critical. This first self-sustaining chain reaction was announced to Washington, by telephone, by Arthur Compton who witnessed the event and reported: ‘‘The Italian navigator has just landed in the new world.’’

Fig. 5-11

